Received 16 Sep 2023 | Revised 01 Nov 2023 | Accepted 07 Nov 2023
Vol. 04, No. 02, 19 pages

RESEARCH ARTICLE TUJES Tobruk University Journal of Engineering Sciences

# Modeling and Optimization the Effect of TIG Welding Parameters on the Corrosion Resistance of 2205 DSS Weldments Using Electrochemical Impedance Technique

**Mohamed S. Melad[1], Mohamed Gebril[1], Farag M. Shuaeib[1], Dawod Elabar[1], Farag I. Haidar[1]**

1. Mechanical Engineering Department, Faculty of Engineering, University of Benghazi, Benghazi P.O. Box 1308, Libya

**Abstract.** Duplex stainless steel has a high mechanical properties and good corrosion resistance due to the percentage of alloying elements and the almost equal amount of austenite and ferrite phase. Most DSS applications require welding processes to joint parts together. The carry out welding process affects the microstructure of DSS and leads to formation of the precipitations resulting in poor mechanical properties and corrosion resistance. In this study, the effect of tungsten inert gas TIG welding parameters namely welding current WC, welding speed WS, and $N_2$ addition with Ar as shielding gas on the corrosion resistance have been investigated. The corrosion penetration rate of the DSS weldments determined using electrochemical impedance technique. The response surface methodology was applied in order to achieve the mathematical model that describes the relationship between welding variables and corrosion penetration rate. Results showed that the WC and WS are the most important parameters that affected the corrosion penetration rate. The results clarified that when increasing WC with decreasing WS which means highest heat input the corrosion penetration rate increase due to the appearance of the precipitations; while the decreasing in WC with increasing in WS which means low heat input the corrosion penetration rate also increase due to the increase in ferrite content. The results also found that the addition of a few amount of $N_2$ with Ar as shielding gas leads to decrease the corrosion penetration rate, but when increase the amount of $N_2$ more than 10% leads to increase the corrosion penetration rate due to the reappearance of the precipitations.

Keywords: Duplex stainless steel, TIG welding process, $N_2$ as shielding gas, Response surface method, Electrochemical impedance technique.

## 1. Introduction

The benefit of duplex stainless steel DSS is to have a ferrite microstructure intermixed with austenite makes it have an advantage mechanical properties of ferrite and austenite stainless steel. This combination of microstructure raises their strength, hardness and ductility, and make it has a higher corrosion resistance compared with other stainless steels [1].

DSS containing of nearly equal volume fraction of the austenite and ferrite, performs a good combination of the mechanical properties and corrosion resistance, and has been increasingly used in many industries, such as oceaneering, petrochemical fields, oils and gas, nuclear power engineering[2]–[6]. But its further practical application at high temperature is limited severely due to the inferior thermal stability related to the undesirable precipitations, such as the σ phase and chromium nitrides, which cause a catastrophic of toughness and corrosion resistance [7]–[10]. As a result, the DSS is generally required to serve only below 250-300℃ [11], [12]. Even so, the weld joint of DSS is inevitable for the construction of those engineering structures, which makes the DSS undergo complex thermal recycles and result in severe imbalance of phase ratio and distortion of grain patterns. Moon et al [13] demonstrated the correlation between the sigma phase precipitation and pitting corrosion resistance as well as microstructural change of a super duplex stainless steel welds made by gas tungsten arc (GTA) and they found that the post weld heat treatment temperature at 930 ℃ was a favorable condition to form σ phases. Xie et al [14] studied the microstructure characters and formation mechanism of DSS multi-pass weld joints and they said that the significant phase imbalance was observed at the HAZ and weld fillers, the HAZ became ferritiszation while the austenite was dominating at weld fillers. Consequently, the DSS weld joints are always the weakest link to threaten the structure integrity of those engineering components, particularly in the circumstances related to the strength and hardness that is highly susceptible to the microstructure characteristics. Thus, it is of great scientific and engineering significance to clarify the microstructure formation and its correlation with the corrosion resistance of DSS weldments.

Duplex stainless steels generally demonstrate good weldability, but the formation of excessive ferrite contents, nitrides, and inter-metallic phases in the weld metal and heat affected zone (HAZ) can occur[15]. Recommendations[16], accordingly, have been established for welding DSS, for example to use limited heat inputs, filler metals with promoted nickel content, nitrogen containing shielding in TIG welding. Ravichandran et al. [17] studied the effect of Tungsten Inert Gas welding process parameters on mechanical properties of duplex stainless steel (2205) using SN ratio and ANOVA analysis. Welding current, gas flow rate and welding speed were considered as the welding parameters and impact strength and hardness were taken as responses. From the SN ratio analysis, it was concluded that high impact strength can be obtained when the welding current was 150 A, gas

flow rate was 14 L/min and the welding speed was 210 mm/min. Also, the high hardness of the joints could be obtained when the welding current was 190 A, gas flow rate was 12L/min and the welding speed was 175 mm/min. (Ibrahem. Z et al [18] they studied a procedure TIG welding on duplex stainless steel material 2205 with 6mm thickness with_homogeneously 2 passes butt weld joints to find optimum parameters of welding. Four input process parameters (control factors) are considered, namely current welding, welding speed, control feeding rate and argon gas flow rate. The micro-hardness, toughness, and tensile strength of welded joints considered as responses. The welding experiments will be performed according to Taguchi method based on four factors three level design (L3-4). (Design Expert 9) software is used to establish the design matrix and to analyze the experimental data. Furthermore, the developed models were optimized by determining the best combinations of input process parameters in order to produce an excellent weld quality. Results showed that the optimum values of input parameters were (welding current = 198.19 A, welding speed = 146.121 mm/min, gas flow rate = 7 l/min), the responses results were (UTS= 1068.842 MPa, HRD=46.996, IS=91.776 J).

Nitrogen, as one of the strongest austenite forming alloying elements, is an economical and efficient substitute for nickel [19], [20]. It also contributes to high strength and corrosion resistance. If an excessively high content of ferrite forms in the weld metal due to loss of nitrogen during welding it will impair mechanical and corrosion performance of DSS. Du Toit et al.[21], [22] monitored and modeled the absorption and desorption of nitrogen within the molten weld metal of stainless steels. They carried out welding process on various base metals with different nitrogen content in shielding gas. It was cited that the initial contents of nitrogen and surface active elements in the base metal were key factors in controlling the nitrogen loss. Hertzman et al.[23] Also studied nitrogen pick up of 2507-type SDSS and determined the effect of arc length and nitrogen content of the shielding gas. It was said that the nitrogen content of shielding gas and the volume of the weld pool affected the final nitrogen content. Karlsson et al. [13] carried out low heat input autogenously laser welding on 2507 SDSS, which resulted in highly ferritic microstructures with nitride precipitates due to nitrogen loss and high cooling rates. Pimenta et al [24] cited that it is possible to observe an almost linear relationship between the increase in the amount of nitrogen and the volume fraction of austenite in weld metal. Topić & Knezović [25] test the ultimate tensile strength of 2205 duplex stainless steel produced with laser welding and with different combinations of shielding gases and they said that the use of nitrogen in shielding gas should be researched further. Brytan & Niagaj [26] discussed the corrosion characterization of lean duplex stainless steel welded joints using the potentodynamic test and electrochemical impedance spectroscopy in 1 M NaCl solution. Results showed a lower corrosion resistance of TIG and A-TiG, welded joints compared to non-welded parent metal, but introducing heat input properly during welding and applying

shielding gases rich in nitrogen or helium can increase austenitic phase content, which is beneficial for corrosion resistance, and improves surface oxide layer resistance in 1M NaCl solution. Gurrala et al [27] carried out gas tungsten arc welding (GTAW) with different shielding gas compositions to see how the shielding environment affects the protective qualities of passive films of 2205 Duplex stainless-steel (DSS). They implies that the solubility of nitrogen in the weld increases with higher welding heat input and the addition of nitrogen to the shielding gas, resulting in an increase in austenite content that happen during cooling from a welding temperature. It is also observed from the electrochemical impedance spectroscopy (EIS) that the weld zone of activated GTAW with $Ar+N_2$ shielding gas has increased corrosion resistance which is due to the presence of a passive layer on the stainless steel surface, which is exacerbated by the presence of 5% $N_2$ in the argon-nitrogen shielding gas. And finally they said that the weld zone of activated GTAW with $Ar+N_2$ shielding gas has much higher pitting corrosion resistance than GTAW and A-GTAW, which can be attributed to microstructural changes during welding as well as a reduction in active sites of austenite and ferrite interfaces.

Therefore, the aim of this study is to optimize and analysis using response surface methodology the effect of TIG welding process parameters on the corrosion resistance of duplex stainless steel weld joint using electrochemical impedance technique.

## 2. Material and Experimental Procedure

### 2.1 Material and welding process

In this research, the work material used in the experiments is duplex stainless steels 2205 (UNS S32205). The chemical compositions of the base metal (BM) are shown in Table 1. Before welding, the base metal was machined to plates of 6.35×140×50 mm using Abrasive Water Jet cutting machine with double-V butt weld joint and cleaned mechanically in order to remove rusts and containments. The schematic diagram of the welding process is shown in figure 1.

Table 1 Chemical composition of Duplex Stainless Steel

| Component | Cr | Ni | Mn | C | Si | P | Mo | Cu | N | Fe |
|---|---|---|---|---|---|---|---|---|---|---|
| Wt% | 22.2 | 4.70 | 1.72 | 0.03 | 0.037 | 0.03 | 2.55 | 0.2 | 0.17 | 68 |

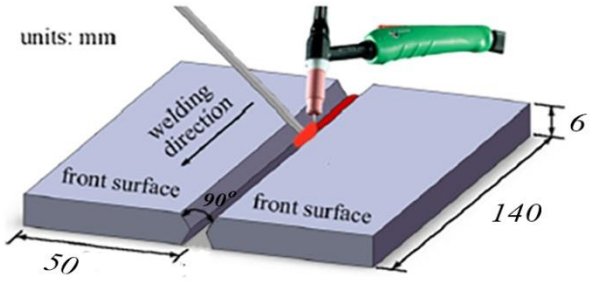


Fig .1 schematic diagram of the welding process

In welding process, the DWHP250NL TIG welding machine was carried out using 2.4 mm tungsten electrode with 8 mm cup size and the constant arc gap was 2 mm. The 1.6 mm filler material that is used in this study was ER2209 and their composition shown in table 2. The filler was manually added to weld pool by welder.

Table 2. The chemical composition of filler material

| components | C | Mn | Si | Cr | Ni | Mo | N | P | S | Fe |
|---|---|---|---|---|---|---|---|---|---|---|
| (wt%) | 0.02 | 1.6 | 0.5 | 23 | 8.5 | 3.1 | 0.11 | >0.01 | <0.005 | Balance |

### 2.2 Experimental Design

Response Surface Method has been adopted for planning the experiments of welding of duplex stainless steel. The experimental design matrix was developed as per central composite rotatable design (CCD) of RSM. Three factors were varied at five levels resulting in a rotatable CCD matrix consisting of 8 cube points, 6 center points in cube and 6 axial points. The input parameters considered in this study are: welding current, welding speed and amount of $N_2$ added to Ar as shielding gas with constant flow rate 10 L/min. 20 butt welded samples have been made using five levels of welding current, welding speed, and amount of $N_2$ added to Ar as shielding gas. The response measured is corrosion rate. The optimization and prediction of the responses were carried out by using response surface design method technique. Based on the trial runs and literature review, the levels of the factors are determined and exhibited in Table 3.

Table 3 the range values of welding process variables

| NO | Input Parameter | levels | | | | |
|---|---|---|---|---|---|---|
| | | -2 | -1 | 0 | 1 | 2 |
| 1 | **Welding current (A)** | **140** | **155** | **170** | **185** | **200** |
| 2 | **Welding speed (mm/min)** | **135** | **155** | **175** | **195** | **215** |
| 3 | **$N_2$ (%)** | **0** | **5** | **10** | **15** | **20** |

After set-up and introducing the factorial levels for each input variable into a MINITAB_19 program, we get the input experiments matrix for the welding processes. Tables 4 demonstrate the matrix of welding processes experiments.

Table 4. The matrix of welding processes experiments

| No | Welding current (A) | Welding speed (mm/min) | $N_2$ % |
|---|---|---|---|
| 1 | **185** | **155** | **15** |
| 2 | **170** | **175** | **10** |
| 3 | **200** | **175** | **10** |
| 4 | **155** | **195** | **15** |
| 5 | **170** | **175** | **0** |
| 6 | **170** | **215** | **10** |
| 7 | **170** | **175** | **10** |

| | | | |
|---|---|---|---|
| 8 | **170** | **175** | **10** |
| 9 | **140** | **175** | **10** |
| 10 | **170** | **175** | **10** |
| 11 | **170** | **175** | **10** |
| 12 | **185** | **195** | **5** |
| 13 | **185** | **195** | **15** |
| 14 | **170** | **175** | **20** |
| 15 | **185** | **155** | **5** |
| 16 | **155** | **195** | **5** |
| 17 | **170** | **135** | **10** |
| 18 | **170** | **175** | **10** |
| 19 | **155** | **155** | **15** |
| 20 | **155** | **155** | **5** |

### 2.3 Electrochemical Impedance Test

Electrochemical Impedance Spectroscopy (EIS) is a well-established quantitative method for the accelerated evaluation of the anti-corrosion performance of protective coatings and the alloys that have a passive film such as stainless steels. Within short testing times, EIS measurements provide reliable data, allowing for the prediction of the long-term performance of the passive film. Electrochemical impedance spectroscopy (EIS) was performed according to ASTM G106 at open circuit potential for 5h and in a 3.5%NACl contains conventional three-electrode cell. The welded specimens were used alternately, as a working electrode (WE); a saturated silver/silver chloride electrode and a graphite rod were used as reference and counter electrode, respectively. The welded samples including weld zone and HAZ were cut to approximation dimensions of 20 mm × 15 mm × 6 mm. In order to supply an electrical connection, a suitable length of copper wire was then spot welded

to one end. After electric connection, the wire was covered by plastic tube and the samples mounted by polystyrene molding epoxy in order to insulate all sides except the area that exposed to the electrolyte. After that, they ground mechanically using a series from 320 to 800 grit SiC emery papers and polished with DP-Lubricant blue and finally they rinsed in distilled water, ultrasonically cleaned by alcohol and then dried in air. EIS measurements were achieved at the open circuit potential for the frequency range of 100 kHz to 10 mHz, using a peak to peak voltage excitation of 10 mV. ACM analysis software with the circuit fit bottom was used to fit the resultant semi circuit nyquist plot to obtain the equivalent circuit and corrosion rate.

## 3. Result and Discussion

The corrosion rate results have been performed using electrochemical impedance technique. The nyquist plot and the equivalent circuit as a result of the electrochemical test of the selected design point have been demonstrated in figure 2.

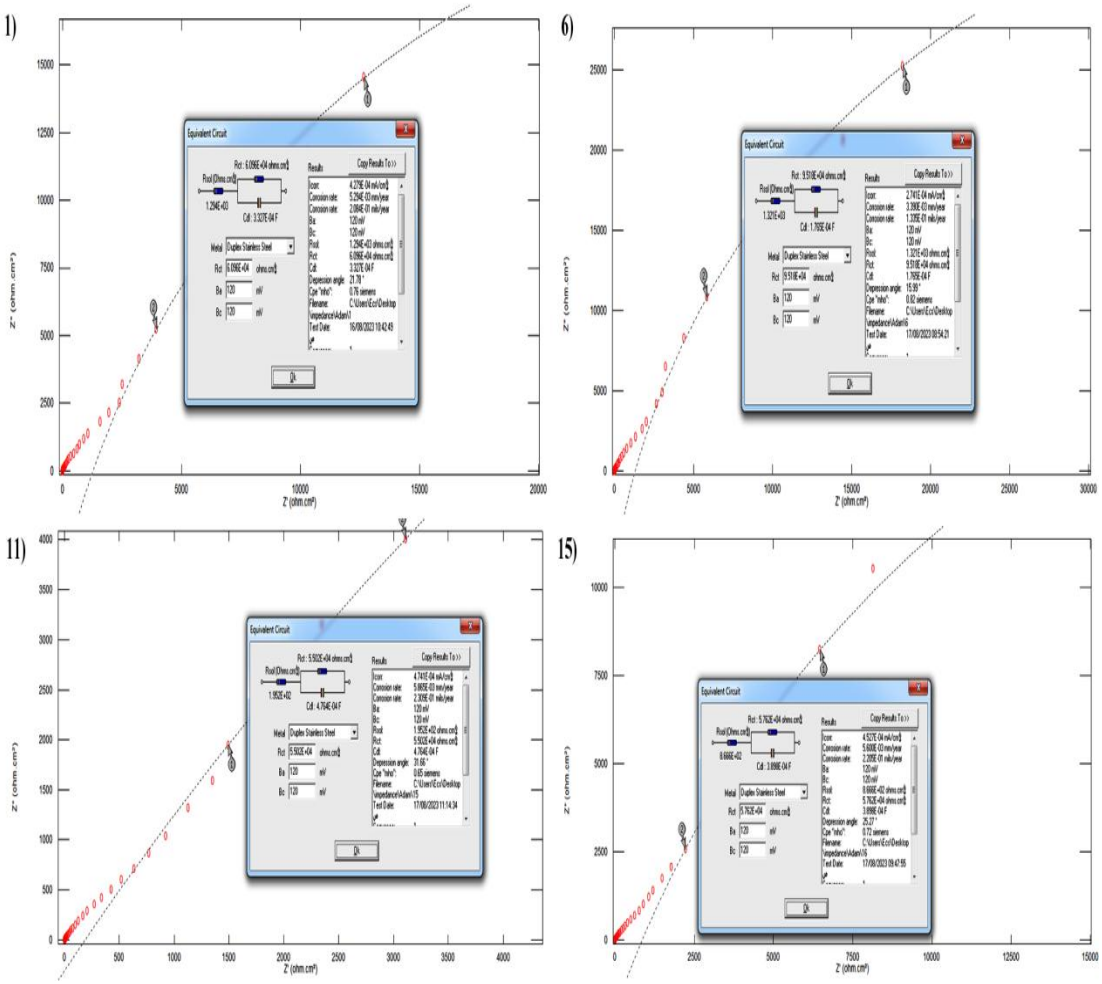


Fig 2. nyquist plot and equivalent circuit of the selected design points

The corrosion penetration rate CPR is the amount of metal lost per year in thickness, the electrochemical impedance spectrum EIS is a powerful technique used to measure the resistance of metals and alloys against corrosion. The corrosion rate of DSS weldments are directly influenced when change in welding parameters. Therefore, it is important to develop a mathematical model to describe the relationship between welding parameters and corrosion rate of DSS weldments. Table 5 represents the welding experiments and the corrosion rate results.

Table 5 experiments and corrosion penetration rate results

| No | Welding Parameters | | | Response |
|---|---|---|---|---|
| | welding current (A) | welding speed (mm/min) | N (%) | $CPR_{EIS}$ mm/y |
| 1 | 185 | 155 | 15 | 0.00525 |
| 2 | 170 | 175 | 10 | 0.00480 |
| 3 | 200 | 175 | 10 | 0.00525 |
| 4 | 155 | 195 | 15 | 0.00480 |
| 5 | 170 | 175 | 0 | 0.00600 |
| 6 | 170 | 215 | 10 | 0.00330 |
| 7 | 170 | 175 | 10 | 0.00460 |
| 8 | 170 | 175 | 10 | 0.00385 |
| 9 | 140 | 175 | 10 | 0.00700 |
| 10 | 170 | 175 | 10 | 0.00365 |
| 11 | 170 | 175 | 10 | 0.00290 |
| 12 | 185 | 195 | 5 | 0.00320 |
| 13 | 185 | 195 | 15 | 0.00180 |
| 14 | 170 | 175 | 20 | 0.00550 |
| 15 | 185 | 155 | 5 | 0.00590 |
| 16 | 155 | 195 | 5 | 0.00550 |
| 17 | 170 | 135 | 10 | 0.00420 |
| 18 | 170 | 175 | 10 | 0.00450 |
| 19 | 155 | 155 | 15 | 0.00440 |
| 20 | 155 | 155 | 5 | 0.00500 |

### 3.1 Analysis of Variance ANOVA of the corrosion

The analysis results for reduced quadratic model for the calculated corrosion rate values are shown in Table 6. In general, if P-values less than 0.05 indicate model terms are significant and values greater than 0.1000 indicate the model terms are not significant. Also, high F value for a parameter means that the parameter has a high effect on the joint characteristics. The terms WS×WS, WC×$N_2$, and WS×$N_2$ have been removed from the mathematical model because they have a high P values 0.414, 0.703,

and 0.666 respectively, which means they have a lowest contribution in this process and also to increase the percentage of Adjusted $R^2$. The model analysis results showed that the WC, WS, WC×WS, and $N_2$×$N_2$ are significant model terms. From table below, it can be noted that the highest F value is at a WC and WS of about 7.98 which means that they have the same effect, while for $N_2$ are equal to 3.04 which means that $N_2$ parameter has less effect on the process. Other model adequacy measures $R^2$ and Adjusted $R^2$ are presented in the table below. The determining factor $R^2$ indicates the goodness of fit of the model. The value of $R^2$ of this model is 82.03%. This implies that at least 82.03% of the variability in the data for the response is explained by the model. This indicates that the proposed model is acceptable.

Table 6 Analysis of variance for corrosion penetration rate

| Source | DF | Adj SS | Adj MS | F-Value | P-Value | |
|---|---|---|---|---|---|---|
| Model | 6 | 0.000023 | 0.000004 | 9.89 | 0.000 | Significant |
| WC (A) | 1 | 0.000003 | 0.000003 | 7.98 | 0.014 | Significant |
| WS (mm/min) | 1 | 0.000003 | 0.000003 | 7.98 | 0.014 | Significant |
| $N_2$ (%) | 1 | 0.000001 | 0.000001 | 3.04 | 0.105 | Not significant |
| $WC^2$ | 1 | 0.000007 | 0.000007 | 17.17 | 0.001 | Significant |
| $N_2^2$ | 1 | 0.000004 | 0.000004 | 11.37 | 0.005 | Significant |
| WC×WS | 1 | 0.000006 | 0.000006 | 15.96 | 0.002 | Significant |
| Error | 13 | 0.000005 | 0.000000 | | | |
| Lack of Fit | 8 | 0.000002 | 0.000000 | 0.60 | 0.755 | Not significant |
| Pure Error | 5 | 0.000003 | 0.000001 | | | |
| Total | 19 | 0.000028 | | | | |
| $R^2$=82.03% | | | | $R^2$ (Adj)=73.74% | | |

### 3.2 Mathematical Model of corrosion

The mathematical model of the corrosion penetration rate CPR of DSS weldments has been developed by linear, square, and interaction regression analysis. It is great to note that the value of each parameter used in this mathematical model should be within the range that presented in table 3. The mathematical equation for CPR has been expressed in terms of the process

variables welding current WC, welding speed WS, and nitrogen addition $N_2$ in the form.

$$CPR = -0.0078 - 0.000276WC + 0.000477WS - 0.000382N_2 + 0.000002WC^2 + 0.000016N_2^2 - 0.000003 \times WC \times WS$$

Where
(CPR) is corrosion penetration rate in (mm/y)
WC is welding current in (A)
WS is welding speed in (mm/min)
$N_2$ in (%)

### 3.3 Three Dimensional Surface and contour Plots

A three dimensional 3D surface plots are used to predict the response value in any given combination of any two parameters, while the third parameter is held at some constant value. In general, if the surface plots reveal much curvature, bend or undulations then the influenced of these combined parameters is high. On other hand, the contour plots are two-dimensional 2D plots, each line/contour in the contour plots represents a constant response line. The 3D surface and contour plots that explained the effect of the change in welding current WC and welding speed WS at constant middle level of $N_2$ on the behavior of CPR value has been presented in figure 3.

From 3D surface plot, it can be clearly seen that at high value of WC the decreasing in WS increases the CPR due to high heat input, while the increasing in WS that relatively lowering the heat input showed reduction in CPR. Moreover, at low value of WC the decreasing in WS that relatively increases the heat input showed reducing in CPR. On other hand, the increasing in WS increased the CPR due to very low heat input that leads to decrease the austenite volume fraction.

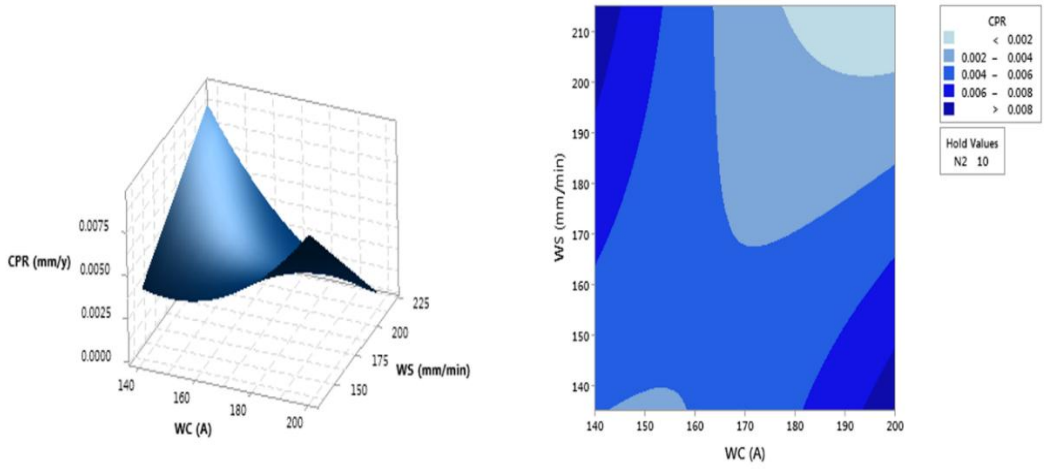


Fig 3. 3D surface and 2D contour plots behavior of CPR versus WC and WS

The contour plot in figure 3 also explained the same behavior as surface plot of the CPR with respect to the change in WC and WS at constant middle level of $N_2$. It can be clearly seen that the both increasing more than 175A in WC with increasing more than 190 mm/min in WS or ranged by 145 to 160 A in WC with decreasing below 140 mm/min in WS leads to a low value of CPR. Since that the very high heat input promotes the increasing in austenite content due to slow cooling rate, but it can also contribute the appearance of the precipitations. Meanwhile, the very low heat input reduced the austenite volume fraction. Knowing that, the corrosion resistance of the austenite phase is higher than the ferrite phase. Therefore, the low value of CPR of DSS weldments can be obtained by performed the appropriate heat input that leads to high austenite content with low amount of the precipitations. However, when changing the amount of the holding $N_2$ value below or more than 10%, the behavior of the CPR with respect to the WC and WS shifted toward high value this is demonstrated in figure 4. Both cases do not effect on the behavior of the 3D surface and contour plots, but there is a change in the CPR values, when increase or decrease the value of $N_2$, the CPR will increase. The reason for increasing CPR when decrease the amount of $N_2$ is the decreasing the amount of austenite phase, while when increasing the amount of $N_2$ more than 10% is the reappearance of the precipitations.

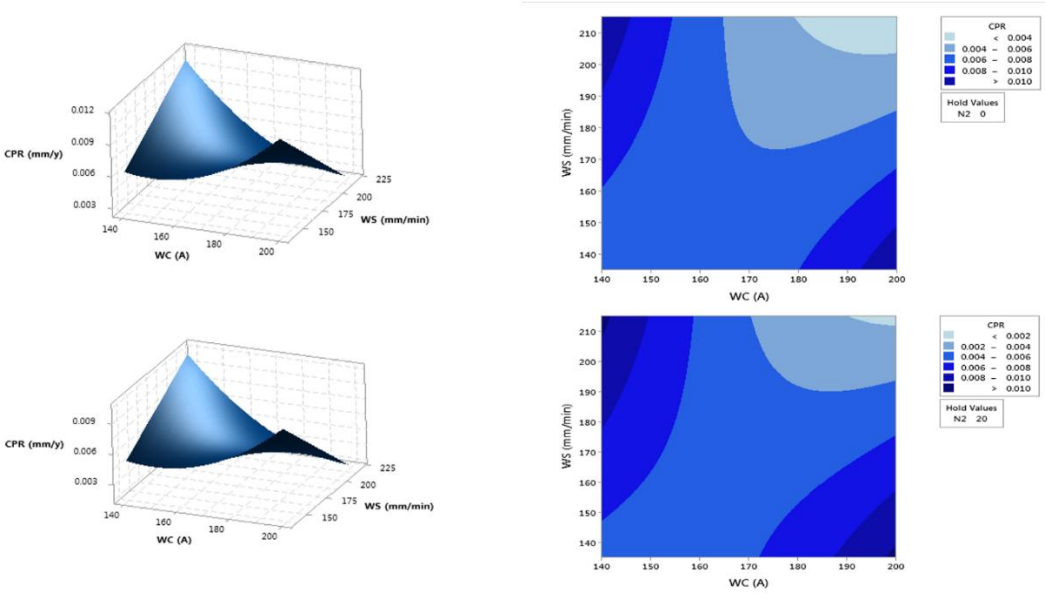


Fig 4. 3D surface and 2D contour plots changing behavior of CPR versus WC and WS at low and high holding values

The 3D surface and contour plots that clarified the effect of change in WC with change in $N_2$ at constant WS on the behavior of CPR has been shown in figure 5. The surface plot illustrated that the decreasing in the value of $N_2$ and WC leads to increase the value of CPR due to an increase in the volume fraction of ferrite phase, which has a low corrosion resistance. On other hand,

the increase in WC with increase the amount of $N_2$ with Ar as shielding gas leads also to increase the CPR. The surface plot also noted that the lowest CPR can be obtained when used a middle value of WC and $N_2$. Since that the addition of $N_2$ with Ar as shielding gas can compensate the N lost from weld pool and increase the driving force of the austenite phase and subsequently decrease the CPR. However, the results of this study showed that when increase the amount of $N_2$, the CPR increased mainly due to the reappearance of the precipitations.

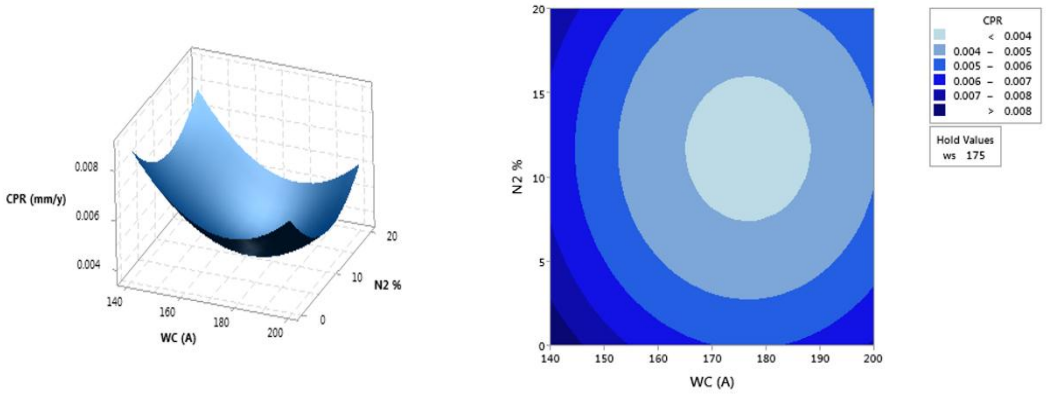


Fig 5. 3D surface and 2D contour plots behavior of CPR versus WC and $N_2$

The contour plot in figure 5 also showed that the lowest value of CPR can obtained when increasing more than 160 A to lower than 190 A in WC, and increasing more than 5% to lower than 15% in $N_2$. Moreover, figure 6 shows the behavior of the CPR with changing in WC and $N_2$ as a surface and contour plots when changing the holding value of WS below and more than middle value. The surface and contour plots illustrated that when reducing the holding value of WS, the CPR increased when increase the value of WC at approximately all values of $N_2$ due to the increasing in heat input that leads to the appearance of the precipitations. On other hand, when increased the holing value of WS the relationship reversed due to the decreasing in heat input that subsequently leads to increase the ferrite volume fraction.

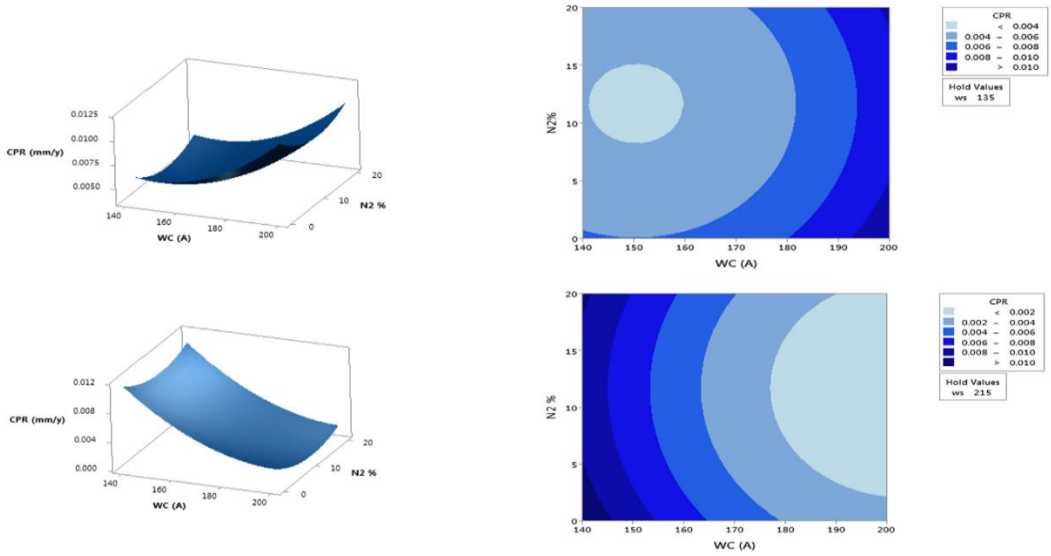


Fig 6. 3D surface and 2D contour plots changing behavior of CPR versus WC and $N_2$ at low and high holding values

The effect of change in WS and $N_2$ at constant WC on the behavior of CPR as a surface and contour plots has been represented in figure 7. From surface plot, it can be seen that at high value of WS, the CPR firstly increased at 100% Ar and then decreased with increase the amount of $N_2$ until reached 10 % $N_2$, more than 10% showed increased trend mainly due to the reappearance of the precipitations.

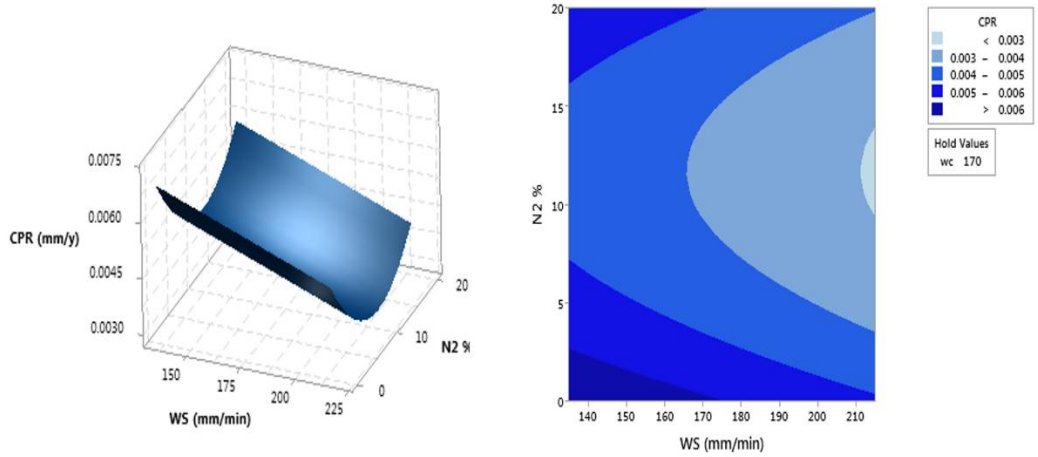


Fig 7. 3D surface and 2D contour plots behavior of CPR versus WS and $N_2$

And also from contour plot showed in figure 7, it can be seen that the high value of WS more than 210 (mm/min) with range between 8 and 13% of $N_2$ decreasing the CPR. And from figure 8 below that shows the behavior of

CPR as a surface and contour plots if the holding value of WC changing below and more than middle value, it can be clearly seen From surface plot that when the WC was 140 A, the decreasing in value of WS with about 10 % of $N_2$ leads to a low value of CPR, while the contour plot showed that the lowest CPR can be obtained when the WS ranges about 175 to 200 mm/min with 10% $N_2$. On other hand, both the surface and contour plots of the holding value of WC more than middle value clarified that the lowest CPR can performed by increased the WS more than 200 mm/min with about 10%$N_2$.

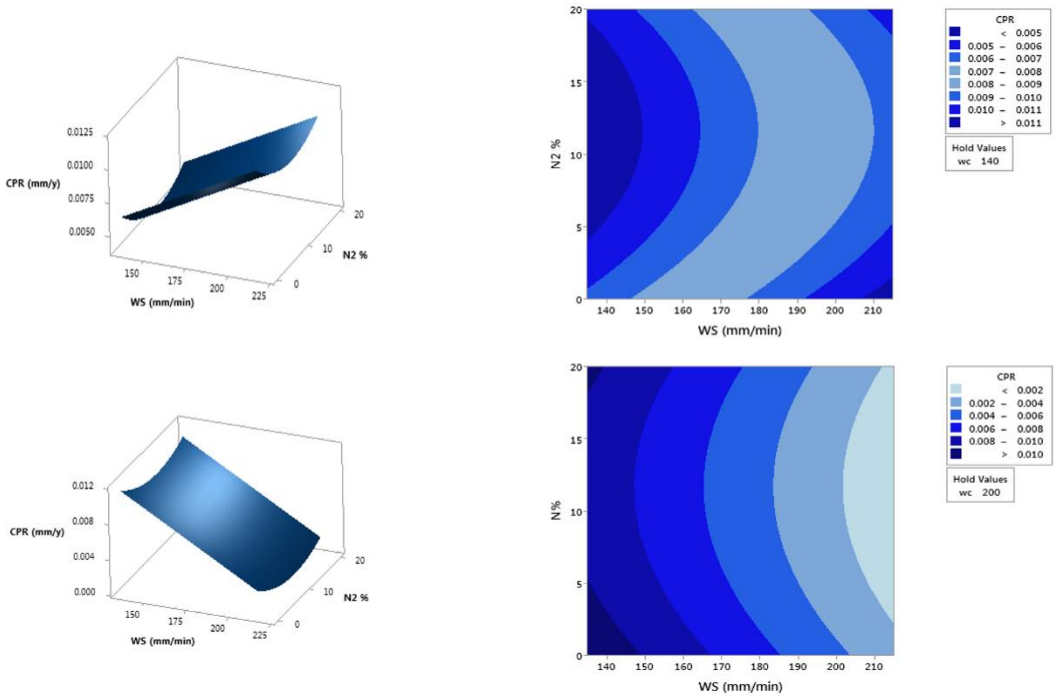


Fig 8.3D surface and 2D contour plots changing behavior of CPR versus WS and $N_2$ at low and high holding values

### 3.4 Optimization plot

The optimization plot shown in figure 9 represents the influence of each parameter on the response. The perpendicular red lines on the plot demonstrate the existing parameter setup and the values in red shown at the top of a column exhibit the existing parameter value settings. The blue dashed line and blue values describe the responses for the existing parameter values. The desirability of this model (D=1) explained the goodness combination of welding parameters satisfies a CPR optimum and are effective at minimizing CPR. From figure 9, it can be noted that the optimum WC, WS, and $N_2$ addition are 200A, 215mm/min, and 12% respectively, which resulted the lowest CPR 0.0005 mm/y. Moreover, the model clearly illustrated that the addition of a few amount of $N_2$ with an appropriate heat input which

performed high austenite content with low amount of precipitation that subsequently leads to a high corrosion resistance of DSS weldments.

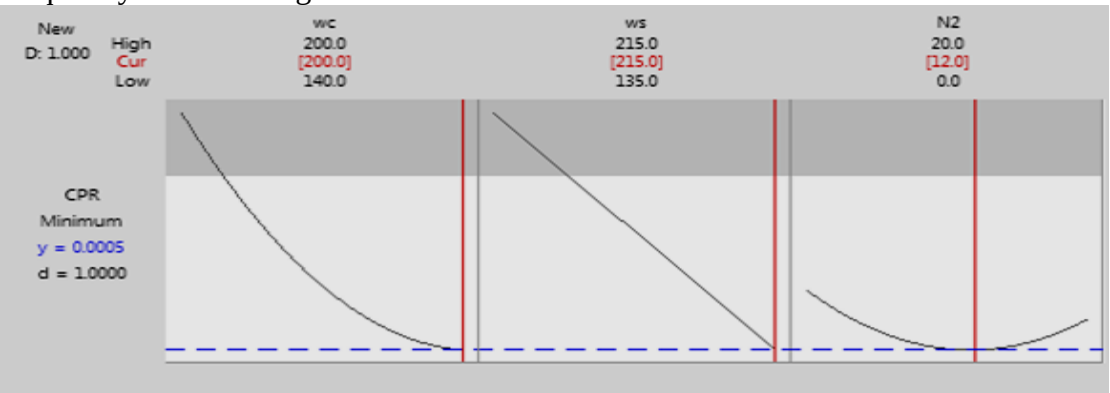


Fig 9. Optimization plot

## 4. Conclusion

In this study, the effect of TIG welding parameters on the corrosion resistance of duplex stainless steel DSS weld joints have been analysed using Response Surface Methodology RSM. The corrosion resistance of DSS weldments explained by corrosion penetration rate and determined using electrochemical impedance spectroscopy (EIS) technique. The main conclusions were presented in the following points:

1. The results proved that the electrochemical impedance technique is a powerful technique used to measure and predict the corrosion penetration rate of DSS weldments
2. The RSM results showed that the welding parameters WC and WS are the significant parameters more than $N_2$ addition on the corrosion penetration rate due to contains lowest P value.
3. The model performed using RSM between welding parameters and corrosion rate of DSS weldments are acceptable due to the 82% of the actual data described by the model.
4. The increasing in WC with decreasing in WS which means high heat input leads to a high value of corrosion penetration rate due to the appearance of precipitations, while the decreasing in WC with increasing in WS which gives low heat input leads also to a high value of corrosion penetration rate due to increasing in ferrite volume fraction.
5. The addition of a few amount of $N_2$ with argon as shielding gas showed that it has benefits on the corrosion resistance of DSS weld joint by decreasing the corrosion penetration rate, while the increase in the amount of $N_2$ leads to an increase in the corrosion penetration rate due to the reappearance of the precipitations.
6. The RSM results showed that the optimum welding parameters WC=200A, WS=215 mm/min, and $N_2$ of about 12% leads to the lowest corrosion penetration rate=0.0005 mm/y.

## References


[1] E. M. Westin, "Microstructure and properties of welds in the lean duplex stainless steel LDX 2101." KTH, 2010.

[2] A. García-Junceda, C. Díaz-Rivera, V. Gómez-Torralba, M. Rincón, M. Campos, and J. M. Torralba, "Analysis of the interface and mechanical properties of field-assisted sintered duplex stainless steels," *Mater. Sci. Eng. A*, vol. 740, pp. 410–419, 2019.

[3] X. Zhang *et al.*, "Microstructure and mechanical properties of TOP-TIG-wire and arc additive manufactured super duplex stainless steel (ER2594)," *Mater. Sci. Eng. A*, vol. 762, p. 138097, 2019.

[4] T. Zhou *et al.*, "Controlled cold rolling effect on microstructure and mechanical properties of Ce-modified SAF 2507 super duplex stainless steel," *Mater. Sci. Eng. A*, vol. 766, p. 138352, 2019.

[5] A. Ameri, Z. Quadir, M. Ashraf, and J. Escobedo-Diaz, "Effects of load partitioning and texture on the plastic anisotropy of duplex stainless steel alloys under quasi-static loading conditions," *Mater. Sci. Eng. A*, vol. 752, pp. 24–35, 2019.

[6] R. Badyka, G. Monnet, S. Saillet, C. Domain, and C. Pareige, "Quantification of hardening contribution of G-Phase precipitation and spinodal decomposition in aged duplex stainless steel: APT analysis and micro-hardness measurements," *J. Nucl. Mater.*, vol. 514, pp. 266–275, 2019.

[7] J. Michalska and M. Sozańska, "Qualitative and quantitative analysis of σ and χ phases in 2205 duplex stainless steel," *Mater. Charact.*, vol. 56, no. 4–5, pp. 355–362, 2006.

[8] H. Sieurin and R. Sandström, "Sigma phase precipitation in duplex stainless steel 2205," *Mater. Sci. Eng. A*, vol. 444, no. 1–2, pp. 271–276, 2007.

[9] G. Fargas, M. Anglada, and A. Mateo, "Effect of the annealing temperature on the mechanical properties, formability and corrosion resistance of hot-rolled duplex stainless steel," *J. Mater. Process. Technol.*, vol. 209, no. 4, pp. 1770–1782, 2009.

[10] R. Badji, M. Bouabdallah, B. Bacroix, C. Kahloun, K. Bettahar, and N. Kherrouba, "Effect of solution treatment temperature on the precipitation kinetic of σ-phase in 2205 duplex stainless steel welds," *Mater. Sci. Eng. A*, vol. 496, no. 1–2, pp. 447–454, 2008.

[11] M. Hättestrand, P. Larsson, G. Chai, J.-O. Nilsson, and J. Odqvist, "Study of decomposition of ferrite in a duplex stainless steel cold worked and aged at 450–500 C," *Mater. Sci. Eng. A*, vol. 499, no. 1–2, pp. 489–492, 2009.

[12] J. C. De Lacerda, L. C. Cândido, and L. B. Godefroid, "Effect of volume fraction of phases and precipitates on the mechanical behavior of UNS S31803 duplex stainless steel," *Int. J. Fatigue*, vol. 74, pp. 81–87, 2015.

[13] I. J. Moon, B. S. Jang, and J. H. Koh, "Heat treatment effect on pitting corrosion of super duplex stainless steel UNS s32750 GTA welds," in

*Advanced Materials Research*, 2013, vol. 746, pp. 467–472. doi: 10.4028/www.scientific.net/AMR.746.467.

[14] X. Xie *et al.*, "Nonhomogeneous microstructure formation and its role on tensile and fatigue performance of duplex stainless steel 2205 multi-pass weld joints," *Mater. Sci. Eng. A*, vol. 786, p. 139426, 2020.

[15] M. Sadeghian, M. Shamanian, and A. Shafyei, "Effect of heat input on microstructure and mechanical properties of dissimilar joints between super duplex stainless steel and high strength low alloy steel," *Mater. Des.*, vol. 60, pp. 678–684, 2014.

[16] L. Karlsson, "Welding of stainless steels. Duplex and superduplex steels," *Weld. Int.*, vol. 14, no. 1, pp. 5–11, 2000.

[17] M. Ravichandran, A. Naveen Sait, and U. Vignesh, "Investigation on TIG welding parameters of 2205 duplex stainless steel," *Int. J. Automot. Mech. Eng.*, vol. 14, no. 3, pp. 4518–4530, Sep. 2017, doi: 10.15282/ijame.14.3.2017.10.0357.

[18] E. M. and F. M. Ibrahem.Z, "Controlling and modelling TIG welding of duplex stainless steel using Taguchi method," University of Benghazi, 2019.

[19] H. Hänninen, J. Romu, R. Ilola, J. Tervo, and A. Laitinen, "Effects of processing and manufacturing of high nitrogen-containing stainless steels on their mechanical, corrosion and wear properties," *J. Mater. Process. Technol.*, vol. 117, no. 3, pp. 424–430, 2001.

[20] J. Li, Z. Ma, X. Xiao, J. Zhao, and L. Jiang, "On the behavior of nitrogen in a low-Ni high-Mn super duplex stainless steel," *Mater. Des.*, vol. 32, no. 4, pp. 2199–2205, 2011.

[21] M. Du Toit and P. C. Pistorius, "Nitrogen control during the autogenous arc welding of stainless steel. Part 2: A kinetic model for nitrogen absorption and desorption," *Weld. J.*, vol. 82, no. 9, pp. 231S-237S, 2003.

[22] M. D. Toit and P. C. Pistorius, "Nitrogen Control during Autogenous Arc Welding of Stainless Steel- Part 1: Experimental Observations.," *Weld. J.*, vol. 82, no. 8, pp. 219–224, 2003.

[23] S. Hertzman, R. J. Pettersson, R. Blom, E. Kivineva, and J. Eriksson, "Influence of shielding gas composition and welding parameters on the N-content and corrosion properties of welds in N-alloyed stainless steel grades," *ISIJ Int.*, vol. 36, no. 7, pp. 968–976, 1996.

[24] A. R. Pimenta, M. G. Diniz, G. Perez, and I. G. Solórzano-Naranjo, "Nitrogen addition to the shielding gas for welding hyper-duplex stainless steel," *Soldag. e Insp.*, vol. 25, pp. 1–8, 2020, doi: 10.1590/0104-9224/SI25.12.

[25] A. Topić and N. Knezović, "31ST DAAAM INTERNATIONAL SYMPOSIUM ON INTELLIGENT MANUFACTURING AND AUTOMATION INFLUENCE OF SHIELDING GAS MIXTURE TYPE ON ULTIMATE TENSILE STRENGTH OF LASER-WELDED JOINTS IN DUPLEX STAINLESS STEEL 2205," 2020, doi: 10.2507/31st.daaam.proceedings.xxx.

[26] Z. Brytan and J. Niagaj, “Corrosion studies using potentiodynamic and EIS electrochemical techniques of welded lean duplex stainless steel UNS S82441,” *Appl. Surf. Sci.*, vol. 388, pp. 160–168, 2016.

[27] A. K. Gurrala, A. Tirumalla, S. Sheik, and R. Mohammed, “Effect of shielding environment on microstructure and corrosion behavior of 2205 duplex stainless-steel weldments”.